Journal of the Neurological Sciences 405 (2019) 116390

Contents lists available at ScienceDirect

Journal of the Neurological Sciences

journal homepage: www.elsevier.com/locate/jns

Evaluation of pituitary structures and lesions with turbo spin-echo diffusion-weighted imaging

Zaw Aung Khant[a], Minako Azuma[a,*], Yoshihito Kadota[a], Youhei Hattori[a], Hideo Takeshima[b], Kiyotaka Yokogami[b], Takashi Watanabe[b], Masahiro Enzaki[c], Takeshi Nakaura[d], Toshinori Hirai[a]

[a] Department of Radiology, University of Miyazaki, Miyazaki, Japan
[b] Department of Neurosurgery, University of Miyazaki, Miyazaki, Japan
[c] Radiology Section, Miyazaki University Hospital, Miyazaki, Japan
[d] Department of Diagnostic Radiology, Graduate School of Medical Sciences, Kumamoto University, Kumamoto, Japan

ARTICLE INFO

Keywords:
Pituitary
Pituitary adenoma.
Magnetic resonance imaging.
Turbo spin-echo diffusion-weighted imaging.
Echo-planar diffusion-weighted imaging.

ABSTRACT

Background and purpose: Turbo spin-echo diffusion-weighted imaging (TSE-DWI) has not been used for evaluating pituitary lesions. We compared the usefulness of TSE-DWI and echo-planar (EP)-DWI for assessing normal pituitary structures and lesions.

Materials and methods: Our study included 41 consecutive patients (27 pituitary adenomas, 8 Rathke's cleft cysts, 4 craniopharyngiomas, 1 germinoma, 1 pituitary metastasis) who underwent conventional pre- and post-contrast magnetic resonance imaging (MRI) and TSE- and EP-DWI at 3T. Two observers independently performed qualitative assessment of normal pituitary structures and lesions on sagittal DWI and apparent diffusion coefficient (ADC) maps. One observer recorded ADC values of normal brain structures and pituitary lesions. Kappa (κ) statistics, Wilcoxon signed-rank test, intraclass correlation coefficient, Bland-Altman analysis, Pearson correlation coefficient and independent *t*-test were used for statistical analysis.

Results: Interobserver agreement for qualitative evaluations was good to excellent (κ = 0.65–1.0). On both DWI and ADC maps, visualization of the pituitary gland, of the spatial relationship between the lesion and its normal surroundings, and the whole image quality were significantly better on TSE- than EP sequences ($p < .01$). In normal brain structures, the ADC value on TSE- and EP-sequences was significantly correlated ($r = 0.6979$, $p < .05$). The TSE-ADC value was significantly lower for pituitary adenomas than craniopharyngiomas ($p < .05$).

Conclusions: For the evaluation of normal pituitary structures and lesions, TSE-DWI is more useful than EP-DWI. The TSE-ADC value may help to differentiate between pituitary adenoma and craniopharyngioma.

1. Introduction

Diffusion-weighted imaging (DWI) and apparent diffusion coefficient (ADC) maps are useful for the evaluation of intracranial diseases including acute cerebral infarction, brain abscess and brain tumors [1–3]. In addition, the clinical usefulness of DWI for pituitary lesions has been reported [4–6]. DWI may provide information about the consistency [4] and prediction of the surgical outcome of macroadenomas [5], and the pretreatment diagnosis of craniopharyngiomas and germ cell tumors to improve the therapeutic outcome [6]. Since it is sometimes difficult to distinguish pituitary adenomas from craniopharyngiomas on conventional MR imaging [7], DWI might help to differentiate them.

Among DWI techniques, an echo-planar (EP) pulse sequence is most commonly used. It involves a primary 90° pulse followed by rephasing gradients instead of repeated 180° degree refocusing pulses (RP). Although EP-DWI may reduce motion-related artifacts and the acquisition time is short, the EP sequence is sensitive to the heterogeneous magnetic field; this results in severe susceptibility artifacts and image distortion [8–10]. Therefore, EP-DWI is not ideal for the evaluation of the skull base and sellar regions because they feature a heterogeneous magnetic field adjacent to the paranasal sinuses and include air.

The turbo spin-echo (TSE) technique is an alternative to DWI. Since the TSE-DWI sequence includes a primary 90° pulse followed by more than one 180° RP [11], it may reduce susceptibility artifacts and image distortion in the regions with a heterogeneous magnetic field.

* Corresponding author at: Department of Radiology, Faculty of Medicine, University of Miyazaki, 5200 Kihara, Kiyotake, Miyazaki 889-1692, Japan.
E-mail address: minako_azuma@med.miyazaki-u.ac.jp (M. Azuma).

https://doi.org/10.1016/j.jns.2019.07.008
Received 1 May 2019; Received in revised form 4 July 2019; Accepted 8 July 2019
Available online 18 July 2019
0022-510X/

Kamimura et al. [9] who studied healthy volunteers showed that TSE-DWI was superior to EP-DWI for the visualization of the normal pituitary gland. Others [8,12] reported that TSE-DWI was more useful than EP-DWI for the diagnosis of pediatric neurological diseases and cholesteatoma. To our knowledge, no systematic comparisons of TSE- and EP-DWI, performed on 3 T magnetic resonance imaging (MRI) systems for the evaluation of pituitary lesions have been published. Therefore, we compared the usefulness of TSE- and EP-DWI for the evaluation of normal pituitary structures and lesions.

2. Material and methods

2.1. Patient population

This retrospective study was approved by our institutional review board, informed patient consent was waived. Using information from electronic medical records, one radiologist (M.A.) selected patients and obtained their MR imaging data from a picture archiving and communication system (PACS) system to prepare the qualitative and quantitative studies. Included were 41 consecutive patients (18 males and 23 females; age range 16–84 years; mean age 60.7 years) with pituitary lesions (27 pituitary adenomas, 8 Rathke's cleft cysts, 4 craniopharyngiomas, 1 germinoma and 1 pituitary metastasis). All patients underwent conventional pre- and post-contrast MRI and TSE- and EP-DWI at 3 T between April 2016 and August 2018; 19 pituitary adenomas and 3 craniopharyngiomas were surgically confirmed. The remaining 19 patients were diagnosed based on their MR imaging findings, follow-up imaging studies, and clinical information.

2.2. MRI protocol

All studies were performed on a 3T MRI system (Philips Ingenia 3T; Philips Medical Systems; Best, The Netherlands) using a 32-channel head coil. All patients underwent conventional pre- and post-contrast-enhanced MRI and TSE- and EP-DWI scanning. MRI included pre-contrast-enhanced sagittal and coronal 2D T1- and T2-weighted (T1-, T2WI) scans and post-contrast-enhanced sagittal and coronal 2D T1-weighted TSE scans. The slice thickness of the T1- and T2-weighted TSE images was 2.5 mm.

Before contrast-enhanced MRI, two types of DWI were performed. The parameters for EP-DWI TR were 3000 ms; TE, 54 ms; field of view (FOV), 170 × 170 mm; matrix, 108 × 108; slice thickness, 3 mm; voxel size, 1.5 × 1.5 × 3.0 mm^3; time of acquisition, 2 min 3 s; average, 4; SENSE factor, 2. For TSE-DWI they were TR, 7000 ms; TE, 56 ms; FOV, 170 × 170 mm; matrix, 108 × 108; slice thickness, 3 mm; voxel size, 1.5 × 1.5 × 3.0 mm^3; time of acquisition, 5 min 50 s; average, 5; SENSE factor, 3.

2.3. Image analysis

2.3.1. Qualitative evaluation

Two observers (T.H. and Z.A.K., with 26 and 3 years of experience with neuro-MRI, respectively) reviewed the sagittal DWI and ADC maps obtained with TSE and EP sequences. The imaging sets were presented on a PACS workstation in random order to the observers who were blinded to the patient identity and to clinical and pathological findings. They independently compared four items with reference to the standard for sagittal contrast-enhanced T1WI, i.e. visualization of the optic chiasm, the pituitary gland, and the pituitary stalk, and the spatial relationship between the lesion and its normal surroundings [13]. They used a 5-point scale where visualization on DWI and ADC maps as clear as on CE-T1WI was scored as excellent (score = 4), structures can be well visible on DWI and ADC maps but are not as clear as on CE-T1WI (good, score = 3), structures can be observed but are obviously vague compared with CE-T1WI (fair, score = 2), structures can be barely recognized on DWI and ADC maps (poor, score = 1), structures cannot be recognized on DWI and ADC maps (nondiagnostic, score = 0). When structures were not visualized on CE-T1WI we performed no further evaluation.

The same two observers also independently recorded the image quality of sagittal DWI and ADC maps obtained with the TSE and EP method. They looked for susceptibility-induced image distortions, blurring and/or SENSE-related artifacts (incomplete unfolding and periodic artifacts) [14]. They used a 5-point score where 1 = non-diagnostic, 2 = poor (substantial artifacts; image distortions or SENSE-related artifacts interfered with the diagnosis in some anatomic parts of the images), 3 = satisfactory (major image distortions or blurring or SENSE-reconstruction artifacts; diagnosis possible in all anatomic regions), 4 = good (minor artifacts, discrete image distortions or some artifacts, no blurring), 5 = excellent (no artifacts). When both readers assigned identical scores the data were collected; when their initial scoring differed, the final score was recorded by consensus.

After the blinded evaluations, both readers consensually compared the signal intensity of the solid part of pituitary adenoma, craniopharyngioma, germinoma and pituitary metastasis with the pons on TSE-DWI and graded it as hypo-, iso-, or hyperintense.

2.3.2. Quantitative evaluation

To calculate the ADC and the signal-to-noise ratio (SNR), regions of interest (ROIs, 20–24 mm^2) were drawn on MRI scans by one observer (Z.A.K.) and cross-referenced with the anatomic structures on T1WI scans. In normal brain structures, ROIs were placed on the splenium of the corpus callosum and the pons on mid-sagittal sections on both ADC maps and DWI scans obtained with the TSE and the EP method. The SNR was calculated as $SNR = SI_{tissue} / SD_{tissue}$, where SI_{tissue} and SD_{tissue} are the signal intensity of tissue and the standard deviation of the signal intensity of tissue, respectively. To show intraobserver reproducibility, the observer performed ADC and SNR measurements for each area, twice, 3 months apart.

To measure TSE-ADC values of pituitary adenoma, craniopharyngioma, germinoma and pituitary metastasis, ROIs (4–5 mm^2) were placed in an enhancing solid portion. Care was taken to avoid cysts, hemorrhages, blood vessels, and areas with visible image distortion/signal loss. To minimize bias, we measured each area 3 times and calculated the average ADC.

2.4. Statistical analysis

Interobserver agreement with respect to the reader-assigned scores was analyzed with the kappa coefficient ($\kappa < 0.20$ = poor-, $\kappa = 0.21$–0.40 = fair-, $\kappa = 0.41$–0.60 = moderate-, $\kappa = 0.61$–0.80 = good-, $\kappa = 0.81$–0.90 = very good-, $\kappa > 0.90$ = excellent agreement). The visual assessment scores and SNRs of the two sequences were compared with the Wilcoxon signed-rank test. To assess the intraobserver reliability of our ADC and SNR measurements, the intraclass correlation coefficient (ICC) was used; ICC < 0.40 = poor, ICC = 0.40–0.59 = fair, ICC = 0.60–0.74 = good, and ICC > 0.74 = excellent. In addition, the intraobserver reliability of the ADC and SNR measurements was analyzed by using the Bland-Altman analysis [15]. Bias and 95% limits of agreement (95% LoA) were calculated. ADC correlations between the two sequences were interpreted with the Pearson correlation coefficient. To compare the TSE-ADC of pituitary adenomas and craniopharyngiomas, the independent *t*-test was used. Differences of $p < .05$ were considered statistically significant.

3. Results

As we excluded 24 optic chiasms, 30 pituitary glands, and 30 pituitary stalks because the structures were not visualized on contrast-enhanced T1W images, 17 optic chiasms, 11 pituitary glands, 11 pituitary stalks, and 41 spatial relationships between lesions and their normal surroundings were included in our qualitative evaluations.

Table 1
Interobserver agreement for the qualitative evaluations.

	TSE-DWI	TSE-ADC	EP-DWI	EP-ADC
Optic chiasm (n = 17)	0.77 (0.58–0.95)	0.79 (0.62–0.96)	0.89 (0.76–1.0)	0.7 (0.49–0.92)
Pituitary gland (n = 11)	0.85 (0.55–1.0)	0.82 (0.52–1.0)	1.0 (1.0–1.0)	1.0 (1.0–1.0)
Pituitary stalk (n = 11)	0.8 (0.56–1.0)	0.65 (0.23–1.0)	0.81 (0.46–1.0)	0.82 (0.6–1.0)
Spatial relationship (n = 41)	0.9 (0.81–1.0)	0.89 (0.78–1.0)	0.94 (0.86–1.0)	1.0 (1.0–1.0)
Whole image quality (n = 41)	0.86 (0.71–1.0)	0.88 (0.71–1.0)	0.86 (0.72–1.0)	0.95 (0.84–1.0)

Note: Data are κ statistics. The 95% confidence interval is shown in parentheses.

Table 2
Comparison of the visualization scores between TSE and EP sequences.

	TSE-DWI vs EP-DWI	p value	TSE-ADC vs EP-ADC	p value
Optic chiasm (n = 17)	2.53 ± 1.07 vs 2.06 ± 1.14	0.0977	3.29 ± 0.99 vs 2.41 ± 1.23	0.0078
Pituitary gland (n = 11)	2.55 ± 0.69 vs 0.18 ± 0.4	0.001	2 ± 1.1 vs 0.45 ± 0.52	0.0039
Pituitary stalk (n = 11)	2.27 ± 0.79 vs 1.18 ± 1.33	0.0625	2.45 ± 0.52 vs 1.45 ± 1.57	0.0781
Spatial relationship (n = 41)	2.78 ± 0.99 vs 0.71 ± 0.78	< 0.0001	2.98 ± 0.96 vs 0.76 ± 0.73	< 0.0001
Whole image quality (n = 41)	3.59 ± 0.59 vs 1.63 ± 0.54	< 0.0001	3.78 ± 0.52 vs 0.66 ± 0.48	< 0.0001

Note. Values are the mean score ± standard deviation.

3.1. Qualitative evaluation

Interobserver agreement for the qualitative evaluations was good to excellent (κ = 0.65–1.0) (Table 1). Visualization of the optic chiasm was significantly better on TSE-ADC than EP-ADC maps (p = .0078) although there was no significant difference between the two types of DWI scans (Table 2 and Fig. 1). The TSE- was significantly better than the EP sequence for the visualization of the pituitary gland (TSE-DWI vs EP-DWI, p = .001; TSE-ADC map vs EP-ADC map, p = .0039) and for the spatial relationship between the lesion and its normal surroundings (TSE-DWI vs EP-DWI, p < .0001; TSE-ADC map vs EP-ADC map, p < .0001) (Table 2 and Figs. 1–3). For the visualization of the pituitary stalk there was no significant difference between TSE-DWI and EP-DWI and between the TSE-ADC map and EP-ADC map (Table 2 and Fig. 1). For the whole image quality, the TSE- was significantly superior to the EP sequence (p < .0001) (Table 2 and Figs. 1–3).

The signal intensities of pituitary lesions on TSE-DWI compared with the pons are shown in Table 3. In 27 pituitary adenomas, the

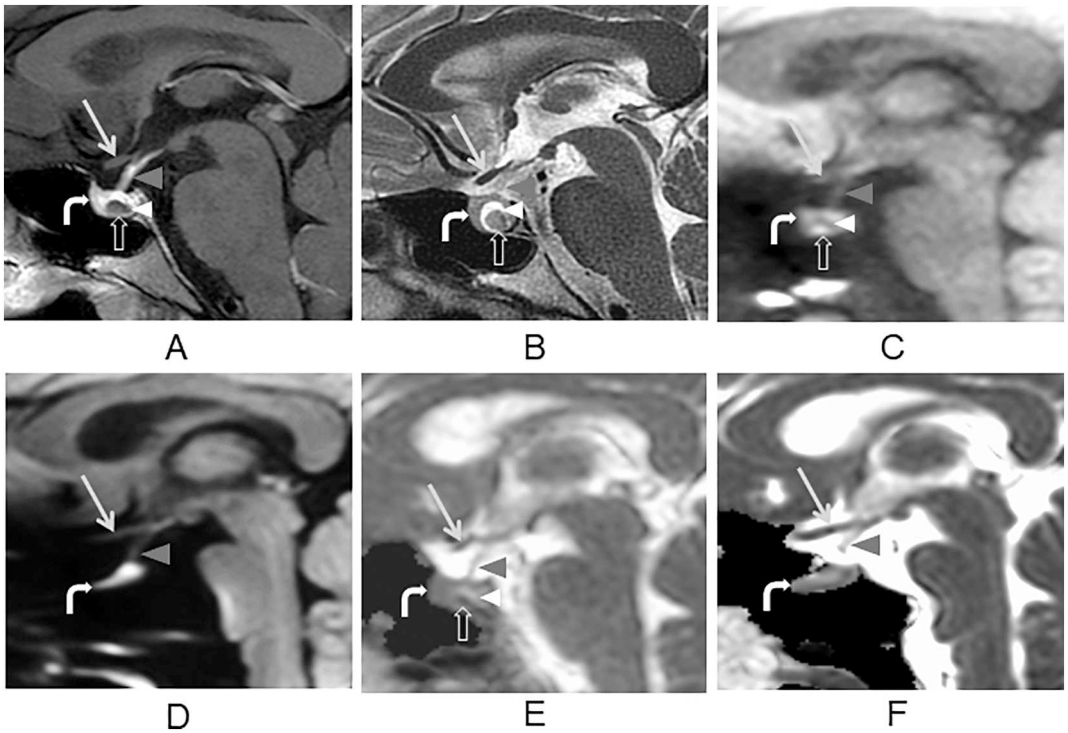

Fig. 1. A 51-year-old woman with Rathke's cleft cyst.
(A) contrast-enhanced T1-weighted image, (B) T2-weighted image, (C) TSE-DW image, (D) EP-DW image, (E) TSE-ADC map, (F) EP-ADC map.
A cystic area (white arrowhead) is seen in the pituitary gland on (A) and (B); an intracystic nodule (open arrow) is isointense to normal pituitary gland on (B), slightly hyperintense on (C), and slightly hypointense on (E). Visualization of the pituitary gland (curved arrow) and the optic chiasm (arrow) on (C) and (E) is similar on (A), while their visualization on (D) and (F) is different due to severe image distortion. The visualization of the pituitary stalk (gray arrowhead) is similar on (C), (D) and (E) except (F). The spatial relationship between the cystic lesion (white arrowhead) and its normal surroundings are better visualized on (C) and (E). A score of 3 was assigned to both scans. The whole image quality was significantly better on TSE (C and E, score 4 each) than EP sequences (D and F, score 2 each).

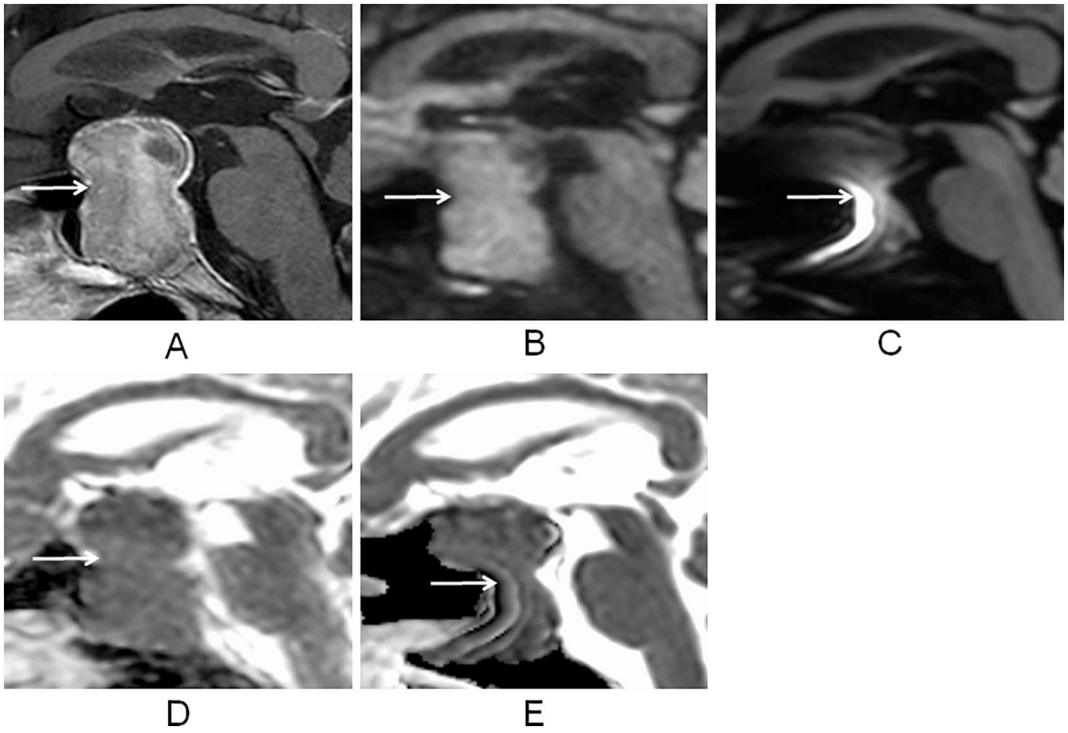

Fig. 2. A 76-year-old woman with pathologically proven pituitary adenoma.
(A) contrast-enhanced T1-weighted image.
(B) TSE-DW image.
(C) EP-DW image.
(D) TSE-ADC map.
(E) EP-ADC map.
Compared to (A), the spatial relationship between the pituitary adenoma (arrow) and its normal surroundings can be clearly identified on (B) and (D). The assigned score was 4 for (B) and (D). It is not well depicted on (C, score 1) and (E, score 1) due to severe image distortion. The whole image quality was significantly better on TSE (B and D, score 4 each) than EP sequences (C and E, score 2 each). The average TSE-ADC value for the pituitary adenoma was $0.64 \times 10^{-3}\,mm^2/s$.

signal intensities were hyperintense in 16 (59.3%), isointense in 8 (29.6%) and hypointense in 3 (11.1%). For 4 craniopharyngiomas, they were hyperintense in 1 (25%) and hypointense in 3 (75%). The 1germinoma and 1 pituitary metastasis revealed isointensity and hypointensity, respectively.

3.2. Quantitative evaluation

The ICC with a 95% confidence interval for intraobserver agreement in ADC and SNR was good to excellent; it was 0.68 with 0.54–0.78 for EP-ADC value, 0.73 with 0.6–0.81 for TSE-ADC value, 0.84 with 0.76–0.89 for EP-SNR and 0.7 with 0.57–0.89 for TSE-SNR (Table 4). For intraobserver reliability of ADC and SNR, the bias with a 95% LoA was 0.01 with −0.05-0.07 for EP-ADC value, −0.001 with −0.07-0.07 for TSE-ADC value, −0.2 with −11.36-10.95 for EP-SNR and − 0.65 with −12.8-11.51 for TSE-SNR (Table 4 and Fig. 4). With regard to normal brain structures, there was a significant correlation in the ADC of the TSE- and EP-sequences ($r = 0.6979$, $p < .0001$) although it tended to be slightly higher for TSE- than EP-sequences (Fig. 5). There was no significant difference in the SNR of TSE-DWI (mean ± standard deviation, 25.34 ± 7.42) and EP-DWI (26.16 ± 9.64) (p = .837). The TSE-ADC was significantly lower for pituitary adenomas (mean ± standard deviation, $0.69 \pm 0.15 \times 10^{-3}\,mm^2/s$) than craniopharyngiomas (mean ± standard deviation,$1.02 \pm 0.27 \times 10^{-3}\,mm^2/s$) (p = .0007) (Table 3 and Figs. 2, 3). The mean TSE-ADCs ± standard deviation of germinoma and pituitary metastasis were $0.79 \pm 0.03 \times 10^{-3}\,mm^2/s$ and $1.06 \pm 0.03 \times 10^{-3}\,mm^2/s$, respectively (Table 3).

4. Discussion

Our qualitative evaluation showed that TSE-DWI was superior to EP-DWI with respect to the visualization of the pituitary gland, the assessment of the spatial relationship between the lesion and its normal surroundings, and the whole image quality. We also found that interobserver agreement was good to excellent although the experience of the two readers with neuro-MRI was quite different (26 vs 3 years). Based on our findings we suggest that, regardless of the reader's experience, TSE-DWI is an effective method for reducing artifacts and improving the quality on images obtained to interpret pituitary lesions.

Studies reported by others found that TSE-DWI was superior to EP-DWI for the evaluation of pathologies other than pituitary lesions and of the normal pituitary gland. According to Elefante et al. [12], in their 32 patients, TSE-DWI was more sensitive than EP-DWI (79–100% vs 75–96%) and more specific (37.5–87% vs 25–75%) for the diagnosis of cholesteatoma. Pokorney et al. [8] preferred TSE-DWI to EP-DWI for the diagnosis of 15 patients with pediatric neurological diseases because it yielded a better diagnostic image quality and fewer clinically relevant artifacts. Kamimura et al. [9] also reported that the normal pituitary gland was clearly visualized on TSE-DWI and undetectable on EP-DWI scans. However, they visually assessed the pituitary gland only on DWI scans of 8 healthy volunteers. Our study, on the other hand, performed visual assessment of not only the pituitary gland but also of other normal anatomical structures, examined the spatial relationship between the lesion and its normal surroundings, and graded the whole image quality on both DWI scans and ADC maps of patients with pituitary lesions.

Our quantitative evaluation of normal brain structures showed that

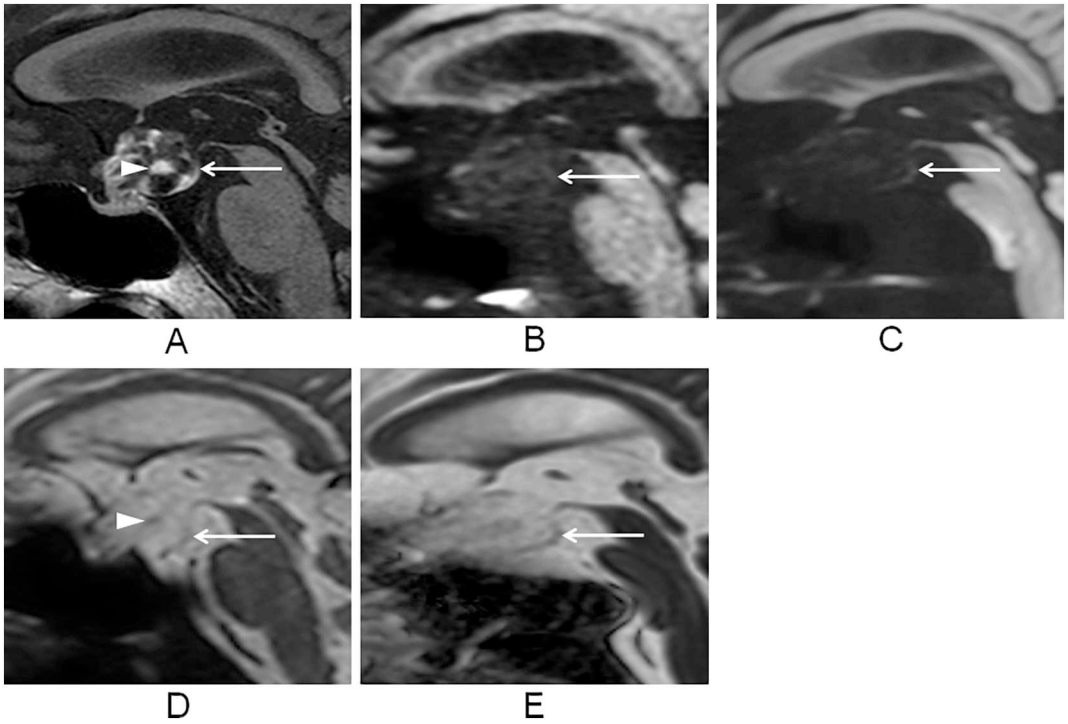

Fig. 3. An 80-year-old man with pathologically proven craniopharyngioma.
(A) contrast-enhanced T1-weighted image.
(B) TSE-DW image.
(C) EP-DW image.
(D) TSE-ADC map.
(E) EP-ADC map.
Compared to (A), the spatial relationship between the craniopharyngioma (arrow) and its normal surroundings can be barely identified on (B, score 2) and (D, score 2). It is not recognizable on (C, score 0) and (E, score 0) due to severe image distortion. The whole image quality was significantly better on TSE sequences (B, score 3) and (D, score 4) than on EP sequences (C and E, score 1). The average TSE-ADC value of the enhancing solid part of the craniopharyngioma (arrowhead) was $1.37 \times 10^{-3}\,mm^2/s$.

Table 3
Summary of TSE-DWI signal intensity and TSE-ADC value of pituitary solid lesions.

	Pituitary adenoma (n = 27)	Craniopharyngioma (n = 4)	Germinoma (n = 1)	Pituitary metastasis (n = 1)
DWI signal intensity				
Hyperintensity	16	1	0	0
Isointensity	8	0	1	0
Hypointensity	3	3	0	1
ADC value*	0.69 ± 0.15[a]	1.02 ± 0.27[a]	0.79 ± 0.03	1.06 ± 0.03

Note. *ADC values are presented as "$\times 10^{-3}\,mm^2/s$" and the mean ± standard deviation.
[a] There was a significant difference in mean ADC value between pituitary adenoma and craniopharyngioma ($p < .05$).

Table 4
Intraobserver reproducibility of ADC and SNR measurements in normal brain tissues.

	ICC	Bias	95% limits of agreement
EP-ADC	0.68 (0.54–0.78)	0.01	−0.05-0.07
TSE-ADC	0.73 (0.6–0.81)	−0.001	−0.07-0.07
EP-SNR	0.84 (0.76–0.89)	−0.2	−11.36-10.95
TSE-SNR	0.7 (0.57–0.89)	−0.65	−12.8-11.51

Note. Data in parentheses show 95% confidence interval.

the ADC of both sequences was significantly correlated although it tended to be slightly higher for TSE- than EP-sequences. In other studies also [10,16], the ADC was higher on TSE- than EP-DWI scans. In our assessment of normal brain structures, the effect of image artifacts may have been negligible because ADC measurements were performed in areas with few susceptibility artifacts. Since the signal intensity on DWI directly affects the ADC value {[ADC = l n (S_0/S_1) / $(b_1 - b_0)$], where S_0 and S_1 are the signal intensity and b_0 *and* b_1 are the b value}, the difference in the signal intensity on TSE- and EP-ADC maps may have affected our ADC values.

The usefulness of quantitative parameters for EP-DWI and of the FOV on optimized and constrained, undistorted single-shot (FOCUS)-DWI scans has been shown in patients with pituitary lesions. Pierallini et al. [4] concluded that in their 22 patients, the EP-ADC value yielded information on macroadenomas. In a more recent study [17] it was shown that in 56 study subjects the FOCUS-ADC value of macroadenomas was significantly lower than of the normal pituitary gland. Lee et al. [6] reported that on DWI scans, the signal intensity of germ cell tumors (n = 12) was significantly higher than of craniopharyngiomas (n = 17). However, they did not evaluate the ADC of the lesions. Ours is the first documentation that the TSE-ADC value of pituitary adenomas was significantly lower than of craniopharyngiomas. Differentiation between pituitary adenomas and craniopharyngiomas

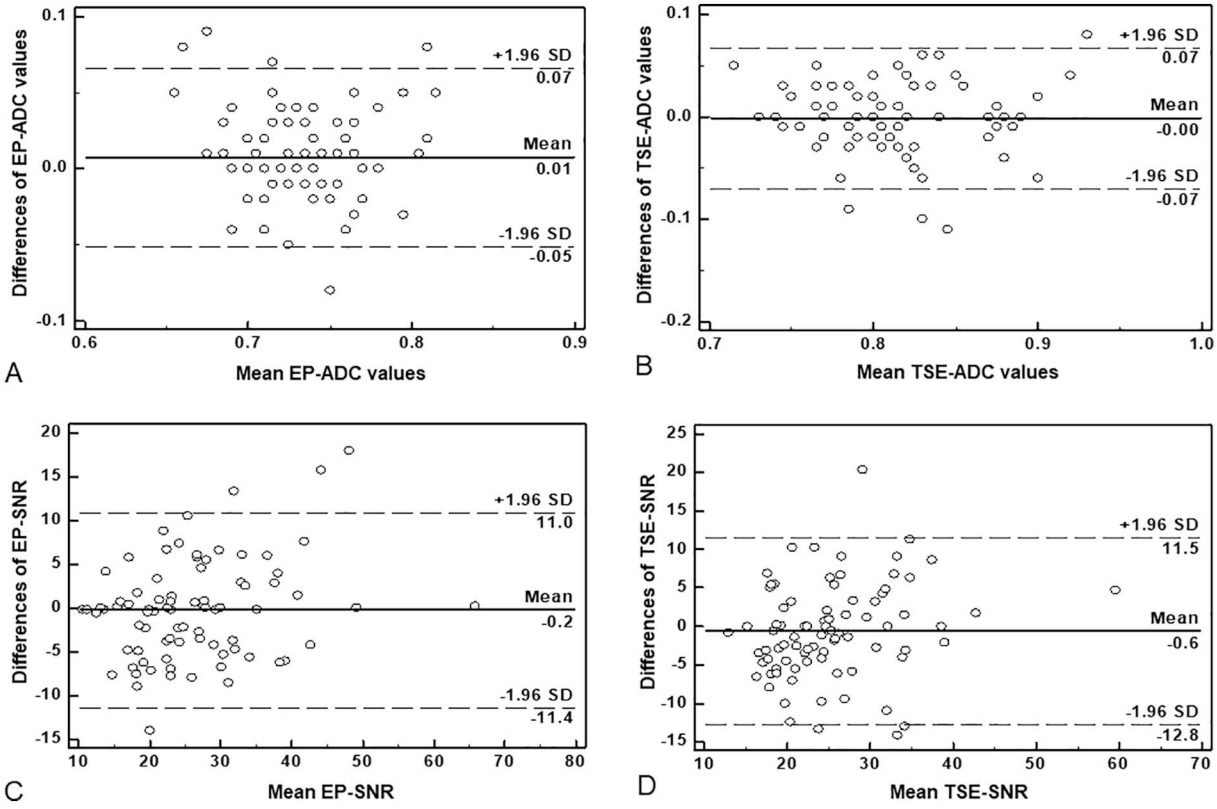

Fig. 4. Bland-Altman plots showing intraobserver variability for (A) EP-ADC value, (B) TSE-ADC value, (C) EP-SNR and (D) TSE-SNR in normal brain tissues. Solid lines indicate mean absolute differences (ie, bias); dashed lines, 95% limits of agreement.

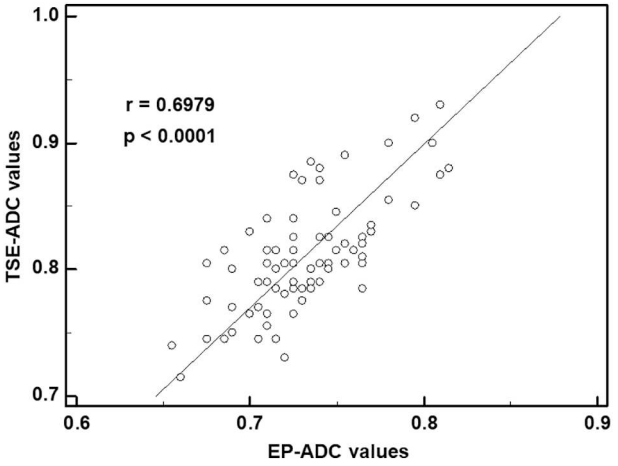

Fig. 5. The Pearson correlation coefficient between TSE- and EP-ADC values ($\times 10^{-3}$ mm^2/s) in normal brain tissue.

may sometimes be difficult on conventional MRI because there may have some overlapping MRI findings between these two lesions [7]. Based on our results, we suggest that TSE-ADC may aid in the differentiation of these lesions.

Mikayama et al. [10] recently reported that at 3 T, the SNR was significantly higher on TSE- than EP-DWI scans of head and neck regions. In earlier 1.5 T MRI studies it was found to be lower on TSE- than EP-DWI scans [16,18]. We cannot explain the discrepancy between our and earlier findings but suspect that it is due to the difference in the examined anatomical structures, the MR sequence parameters and the MRI scanners.

There were some disadvantages of TSE-DWI compared to EP-DWI in our study. First, the SNR of TSE-DWI was relatively lower than that of EP-DWI in our result although there was no significant difference. Second, the acquisition time of TSE-DWI (5 min 50 s) was longer than that of EP-DWI (2 min 3 s). Therefore, TSE-DWI could be more sensitive to the motion-related artifacts compared to EP-DWI. However, in our study, these artifacts were not apparently observed on TSE-DWI.

At present, pituitary lesions tend to be diagnosed on CE-MRI scans [19]. However, gadolinium-based contrast agents can elicit nephrogenic systemic fibrosis in patients with advanced chronic kidney disease or acute renal failure [20]. Therefore, to characterize pituitary lesions in patients with impaired renal function or allergic reactions to contrast agents, the acquisition of TSE-DWI may be useful.

Our retrospective study has some limitations. First, our patient population was relatively small and performed at a single institution. Second, pathological disease confirmation was available for only 19 of 27 pituitary adenomas and 3 of 4 craniopharyngiomas. Nonetheless, our findings warrant further multicenter studies on large populations.

5. Conclusions

Based on our preliminary study, TSE-DWI is more useful than EP-DWI for the evaluation of normal pituitary structures and lesions. The TSE-ADC value may be a helpful parameter for differentiating pituitary adenomas from craniopharyngiomas.

References

[1] E. Tong, Q. Hou, J.B. Fiebach, M. Wintermark, The role of imaging in acute ischemic stroke, Neurosurg. Focus. 36 (2014) E3.
[2] X.X. Xu, B. Li, H.F. Yang, Y. Du, Y. Li, W.X. Wang, H.J. Zheng, Q.Y. Gong, Can diffusion-weighted imaging be used to differentiate brain abscess from other ring-enhancing brain lesions? A meta-analysis, Clin. Radiol. 69 (2014) 909–915.
[3] S.E. Maier, Y. Sun, R.V. Mulkern, Diffusion imaging of brain tumors, NMR Biomed. 23 (2010) 849–864.
[4] A. Pierallini, F. Caramia, C. Falcone, E. Tinelli, A. Paonessa, A.B. Ciddio, M. Fiorelli, F. Bianco, S. Natalizi, L. Ferrante, L. Bozzao, Pituitary macroadenomas:

preoperative evaluation of consistency with diffusion-weighted MR imaging - initial experience, Radiology 239 (2006) 223–231.
[5] J.L. Boxerman, J.M. Rogg, J.E. Donahue, J.T. Machan, M.A. Goldman, C.E. Doberstein, Preoperative MRI evaluation of pituitary macroadenoma: imaging features predictive of successful transsphenoidal surgery, AJR Am. J. Roentgenol. 195 (2010) 720–728.
[6] H.J. Lee, C.C. Wu, H.M. Wu, S.C. Hung, J.F. Lirng, C.B. Luo, F.C. Chang, W.Y. Guo, Pretreatment diagnosis of suprasellar papillary craniopharyngioma and germ cell tumors of adult patients, AJNR Am. J. Neuroradiol. 36 (2015) 508–517.
[7] S.H. Choi, B.J. Kwon, D.G. Na, J.H. Kim, M.H. Han, K.H. Chang, Pituitary adenoma, craniopharyngioma, and Rathke cleft cyst involving both intrasellar and suprasellar regions: differentiation using MRI, Clin. Radiol. 62 (2007) 453–462.
[8] A.L. Pokorney, J.H. Miller, H.H. Hu, Comparison of 2D single-shot turbo-spin-echo and spin-echo echo-planar diffusion weighted brain MRI at 3.0 tesla: preliminary experience in children, Clin. Imaging 42 (2017) 152–157.
[9] K. Kamimura, M. Nakajo, Y. Fukukura, T. Iwanaga, T. Saito, M. Sasaki, T. Fujisaki, A. Takemura, T. Okuaki, T. Yoshiura, Intravoxel incoherent motion in normal pituitary gland: initial study with turbo spin-echo diffusion-weighted imaging, AJNR Am. J. Neuroradiol. 37 (2016) 2328–2333.
[10] R. Mikayama, H. Yabuuchi, S. Sonoda, K. Kobayashi, K. Nagatomo, M. Kimura, S. Kawanami, T. Kamitani, S. Kumazawa, H. Honda, Comparison of intravoxel incoherent motion diffusion-weighted imaging between turbo spin-echo and echo-planar imaging of the head and neck, Eur. Radiol. 28 (2018) 316–324.
[11] D.C. Alsop, Phase insensitive preparation of single-shot RARE: application to diffusion imaging in humans, Magn. Reson. Med. 38 (1997) 527–533.
[12] A. Elefante, M. Cavaliere, C. Russo, G. Caliendo, M. Marseglia, D. Cicala, D. Piccolo, A. Di Lullo, L. Brunetti, A. Palma, M. lengo, A. Brunetti, Diffusion weighted MR imaging of primary and recurrent middle ear cholesteatoma: an assessment by readers with different expertise, Biomed. Res. Int. 2015 (2015) 597896.
[13] L. Yiping, L. Hui, Z. Kun, G. Daoying, Y. Bo, Diffusion-weighted imaging of the sellar region: a comparison study of BLADE and single-shot echo planar imaging sequences, Eur. J. Radiol. 83 (2014) 1239–1244.
[14] C.K. Kuhl, J. Gieseke, M. von Falkenhausen, J. Textor, S. Gernert, C. Sonntag, H.H. Schild, Sensitivity encoding for diffusion-weighted MR imaging at 3.0 T: Intraindividual comparative study, Radiology 234 (2005) 517–526.
[15] J.M. Bland, D.G. Altman, Statistical methods for assessing agreement between two methods of clinical measurement, Lancet 1 (1986) 307–310.
[16] A.S. Kolff-Gart, P.J. Pouwels, D.P. Noij, R. Ljumanovic, V. Vandecaveye, F. de Keyzer, R. de Bree, P. de Graaf, D.L. Knol, J.A. Castelijns, Diffusion weighted imaging of the head and neck in healthy subjects: reproducibility of ADC values in different MRI systems and repeat sessions, AJNR Am. J. Neuroradiol. 36 (2015) 384–390.
[17] M. Wang, H. Liu, X. Wei, C. Liu, T. Liang, X. Zhang, C. Jin, X. Li, Q. Sun, H. Jiang, J. Yang, Application of reduced-FOV diffusion-weighted imaging in evaluation of normal pituitary glands and pituitary macroadenomas, AJNR Am. J. Neuroradiol. 39 (2018) 1499–1504.
[18] J. Sakamoto, Y. Sasaki, M. Otonari-Yamamoto, T. Sano, Comparison of various methods for quantification of apparent diffusion coefficient of head and neck lesions with HASTE diffusion-weighted MR imaging, Oral Surg. Oral Med. Oral Pathol. Oral Radiol. 114 (2012) 266–276.
[19] M.C. Rossi Espagnet, L. Bangiyev, M. Haber, K.T. Block, J. Babb, V. Ruggiero, F. Boada, O. Gonen, G.M. Fatterpekar, High-resolution DCE-MRI of the pituitary gland using radial k-space acquisition with compressed sensing reconstruction, AJNR Am. J. Neuroradiol. 36 (2015) 1444–1449.
[20] L. Daftari Besheli, S. Aran, K. Shaqdan, J. Kay, H. Abujudeh, Current status of nephrogenic systemic fibrosis, Clin. Radiol. 69 (2014) 661–668.